The International Space Station Solar Alpha Rotary Joint Anomaly Investigation

Elliot P. Harik*, Justin McFatter*, Daniel J. Sweeney**, Carlos F. Enriquez*,
Deneen M. Taylor** and David S. McCann*

Abstract

The Solar Alpha Rotary Joint (SARJ) is a single-axis pointing mechanism used to orient the solar power generating arrays relative to the sun for the International Space Station (ISS). Approximately 83 days after its on-orbit installation, one of the two SARJ mechanisms aboard the ISS began to exhibit high drive motor current draw. Increased structural vibrations near the joint were also observed. Subsequent inspections via Extravehicular Activity (EVA) discovered that the nitrided case-hardened steel bearing race on the outboard side of the joint had extensive damage to one of its three rolling surfaces. A far-reaching investigation of the anomaly was undertaken. The investigation included metallurgical inspections, coupon tests, traction kinematics tests, detailed bearing measurements, and thermal and structural analyses. The results of the investigation showed that the anomaly had most probably been caused by high bearing edge stresses that resulted from inadequate lubrication of the rolling contact. The profile of the roller bearings and the metallurgical properties of the race ring were also found to be significant contributing factors. To mitigate the impact of the damage, astronauts cleaned and lubricated the race ring surface with grease. This corrective action led to significantly improved performance of the mechanism both in terms of drive motor current and induced structural vibration.

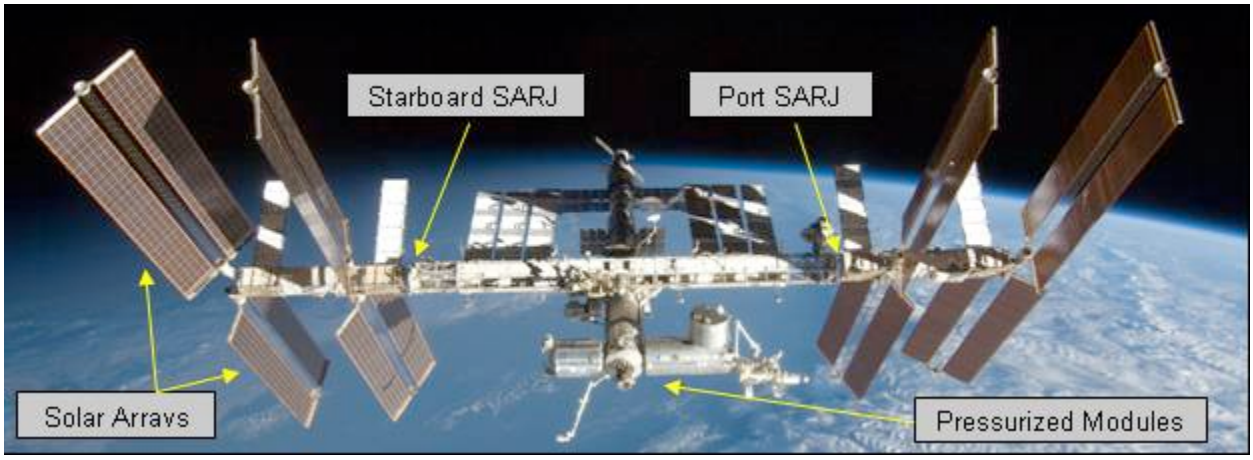

Figure 1. International Space Station as of August 2009

Introduction

International Space Station Overview

The International Space Station (ISS) is a research facility currently being assembled in low Earth orbit. The ISS project is a multi-national effort led by the United States, with partners from Russia, Canada, the European Union, Japan, and others. Construction of the ISS began in 1998 and is scheduled to be complete by 2011 with operations continuing until 2015. The ISS is the largest artificial satellite in Earth

* The Boeing Company, Houston, TX
** NASA Johnson Space Center, Houston, TX

orbit, larger than any previous space station. It was designed as an orbital scientific platform and is intended to operate continuously while supporting a crew of six in pressurized modules. The ISS offers an advantage over spacecraft such as NASA's Space Shuttle because it is a long-term platform in the space environment, allowing scientific experimentation as well as long-duration studies on the human crews that operate them. Long-term expedition crews conduct science daily (approximately 160 man-hours per week), across a wide variety of fields, including human research, life sciences, physical sciences, and Earth observation, as well as education and technology demonstrations. The power required to support the scientific and life sustaining functions of the ISS is provided by arrays of solar panels.

The ISS has a backbone or set of trusses that house several ISS systems. These trusses are joined to a set of pressurized modules that house the crewmembers living and working aboard the ISS. Figure 1 shows the ISS after assembly mission 17A by the Space Shuttle. The pressurized modules are located along the center of the truss structure, extending forward and aft. The power generating solar arrays are located on the port and starboard sides of the truss structure outboard of the SARJs. The location of each Solar Alpha Rotary Joint (SARJ) is indicated in Figure 1.

Solar Alpha Rotary Joint Overview

The SARJ is a single-axis pointing mechanism that allows orbital-rate sun-tracking rotation of the outboard trusses and solar arrays of the ISS. The SARJ completes one full rotation per orbit of the ISS, approximately every 90 minutes. Figure 2 shows a drawing of the SARJ with the major components labeled. The SARJ is capable of transferring 60 kW of electrical power, spare low power (300 W), and data channels across the rotary joint. The total weight of the SARJ is 1161 kg (2561 lb). Two SARJ mechanisms are installed onboard the ISS - Port (activated December 2006) and Starboard (activated June 2007). The SARJ serves as the structural joint between the ISS inboard and outboard truss elements via twelve Trundle Bearing Assemblies (TBA). The trundle bearings straddle between an inboard and outboard triangular cross-section race rings. The race rings are approximately 3.2 meters (10.5 ft) in diameter. TBAs are nominally mounted to the stationary inboard ring while their rollers track against the three surfaces of the outboard race ring. These rollers are highly pre-loaded against the race ring to allow them to react ISS structural loads. The bearing race is made of a 15-5PH stainless steel forging with a nitride hardened case. TBAs are designed for individual on-orbit replacement to protect the mechanism against a roller bearing failure. The SARJ is driven by one of two redundant Drive Lock Assemblies (DLAs) that interface with an integral bull gear on the race ring via a motor-driven pinion. Each DLA is controlled by a Rotary Joint Motor Controller (RJMC) which, in conjunction with processors in the ISS computing infrastructure, performs closed loop control of the joint's motion. SARJ system health and status data is relayed by the processors to the ground in the ISS telemetry stream.

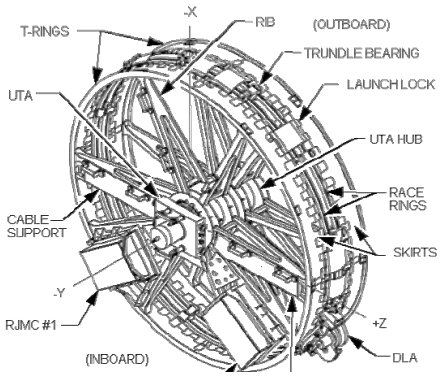

Figure 2. SARJ Overview

Trundle Bearing Assembly Overview

The TBA contains three roller bearing assemblies: two identical upper rollers and a lower, slightly wider, roller. A picture of a TBA is shown in Figure 3. The roller assemblies consist of an internal double row tapered roller bearing whose cup is shrunk fit inside of an outer roller. The outer roller is the physical interface with the SARJ bearing race. The outer roller is made of 440C and is lubricated with 1250-2250 angstroms of gold applied via an ion deposition process. The gold plating on the rollers serves as the sole lubrication scheme for the roller/race interface (the internal tapered roller bearings have a grease lubricant). At the time of the SARJ preliminary design it was believed that the mechanism would be exposed to the atomic oxygen present in the low Earth orbit environment. The final design included thermal shrouds around the entire circumference of the mechanism, but these were not part of the baselined design at the time the lubrication system was being selected. Due to the long life requirement

(30 years) and the assumed exposure of the mechanism to atomic oxygen, lubricant selection criteria of the day [1] led designers to select a metallic film lubricant.

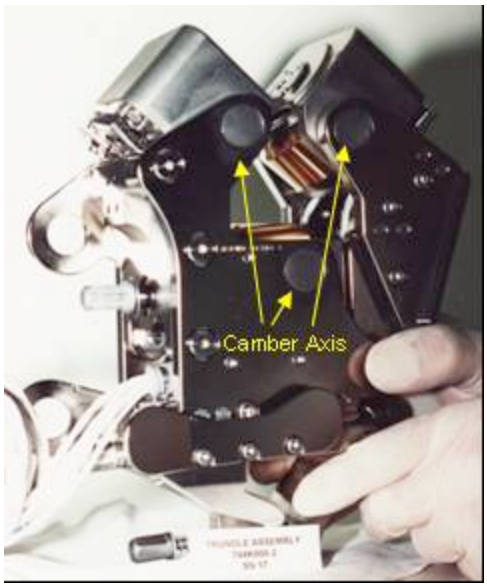

Figure 3. Trundle Bearing Assembly

The roller assembly is fitted into the trundle bearing via a camber pivot axis. This fitting is free to rotate approximately three degrees to allow for proper alignment of the outer roller with the bearing race under mechanical and/or thermal deflections. This rotational axis of the roller assembly leaves the roller susceptible to an overturning moment caused by thrust loads at the roller/race interface. This effect is discussed in detail below. The design intent was that the solid film lubricant on the rollers would mitigate these thrust loads.

On Orbit Anomaly Investigation

Approximately eleven weeks after the Starboard SARJ was activated on-orbit, the mechanism began exhibiting anomalous operational data. For the following two months, engineers on the ground reviewed on-orbit telemetry and worked with the ISS operators and ISS crew to determine the most likely cause of the anomalous signature through a series of on-orbit tests. Eventually, an inspection of the mechanism during an EVA found that the bearing race was damaged and covered in debris.

Initial Anomaly Investigation

The SARJ software provides continuous status on most of the system's performance parameters. These parameters include, but are not limited to, position, speed, motor current draw, target tracking accuracy, and hardware temperatures. This telemetry is reviewed continuously to ensure the health and effective operation of the mechanism. The first indication of anomalous behavior came from unexpected changes in the Starboard SARJ telemetry. In early September 2007, the ISS operations team raised a concern that the difference between the commanded and actual velocity of the SARJ was increasing. The SARJ controller software uses the difference between commanded and actual velocity to determine how much current to provide to the mechanism's drive motor. The change in velocity profile prompted a detailed review of the SARJ operational data. From this review, engineers determined that subtle changes in SARJ performance could be noted starting on September 1st. Figure 4 shows the onset of the anomalous data signature. There are two pieces of telemetry shown. The first is the joint position and the second is the commanded velocity of the mechanism. The three plots depict ten minutes periods of time from three consecutive orbits. Two observations can be made from these data: (1) the irregular data signature initially occurred at a specific angular position of the joint, and (2) the magnitude of the irregularity is

increasing with time. The frequency of the data spikes increased with time such that after a few days the commanded velocity at all SARJ angles was off nominal.

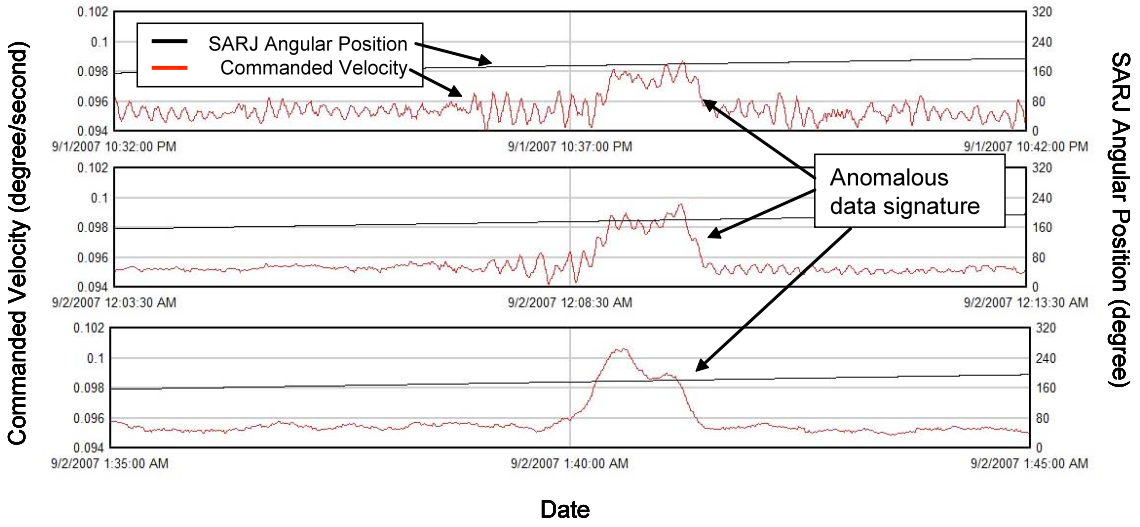

Figure 4. Anomalous Data Signature from the SARJ Controller

This anomalous signature appeared similar to a signature encountered previously on the Port SARJ. The Port SARJ data signature was caused by a problem with the SARJ controller software. With that in mind, the controller and manager software for the system were reset. The intent was to clear out memory buffers and re-initialize controller variables that could be accumulating and leading to the anomalous data signature. The software resets did not lead to any change in the anomalous signature. The SARJ controller did not appear to be the primary cause of the anomaly.

Efforts to exonerate additional components of the system were attempted by switching logical command strings. The SARJ controller architecture utilizes two fully redundant command strings. Each string is composed of a multiplexer/de-multiplexer (MDM) where the SARJ controller software is housed, a RJMC where the velocity control loop and motor power source is located, and a DLA which interfaces with the driven gear of the SARJ and houses the drive motor. Changing commanded strings did not have an appreciable effect on the anomalous data signature. This action demonstrated that the hardware from each drive string was not solely responsible for the data signature.

After clearing the software, MDMs, RJMCs, and DLAs, the primary focus of the investigation turned to the controller logic. While specific anomalies in the software had been ruled out, it was postulated that the controller might be over correcting for slight changes in mechanism performance. If this were the case, then controller parameters could be modified to optimize system performance. A thorough review of the controller logic did not produce any evidence that the anomalous signature could be a controller effect.

Five weeks into the anomaly investigation engineers had eliminated a number of likely causes for the anomaly but still did not understand the root cause. Then a significant change in the drive motor current, approaching system limits, led engineers to the conclusion that the problem was most likely mechanical in nature. An increase in joint drag appeared to be the cause of the anomaly.

Joint Drag Changes During the Anomaly Investigation

The drive motor current is directly related to the torque required to overcome internal drag and applied load in order to rotate the joint. Assuming a benign loading environment, the SARJ torque is a direct measure of the fiction in the joint. The relationship between torque and drive motor current is shown in Equation 1 (torque constant and SARJ gear ratios can be assumed to be constants).

SARJ Torque = Drive Motor Current ● (Torque Constant ● SARJ Gear Ratio) (Eq. 1)

Prior to the anomaly peak motor currents of 0.25 ampere were nominal. This corresponds to joint drag of approximately 790 N·m (590 ft·lbf). During the initial investigation, the peak currents increased to levels as high as 0.60 ampere, or 1910 N·m (1410 ft·lbf) of joint drag. The system capacity is 1.4 amperes. While the increase in drag was over 100% of the nominal value, it was still well within system capacity with a torque margin of 1.33. The drive current readings remained steady for two weeks at the increased level. The system experienced another drastic increase in drive motor current in the first week of October. The multiple changes in drive motor current throughout the course of the investigation are shown in Figure 5. After the 3rd step change drive motor currents were over 1.2 amperes, or 3810 N·m (2810 ft·lbf) of joint drag. In a one week period, the torque margin for the mechanism had decreased from 1.33 to 0.17. There was a risk that with another step change in required current there would be an unrecoverable stall of the mechanism.

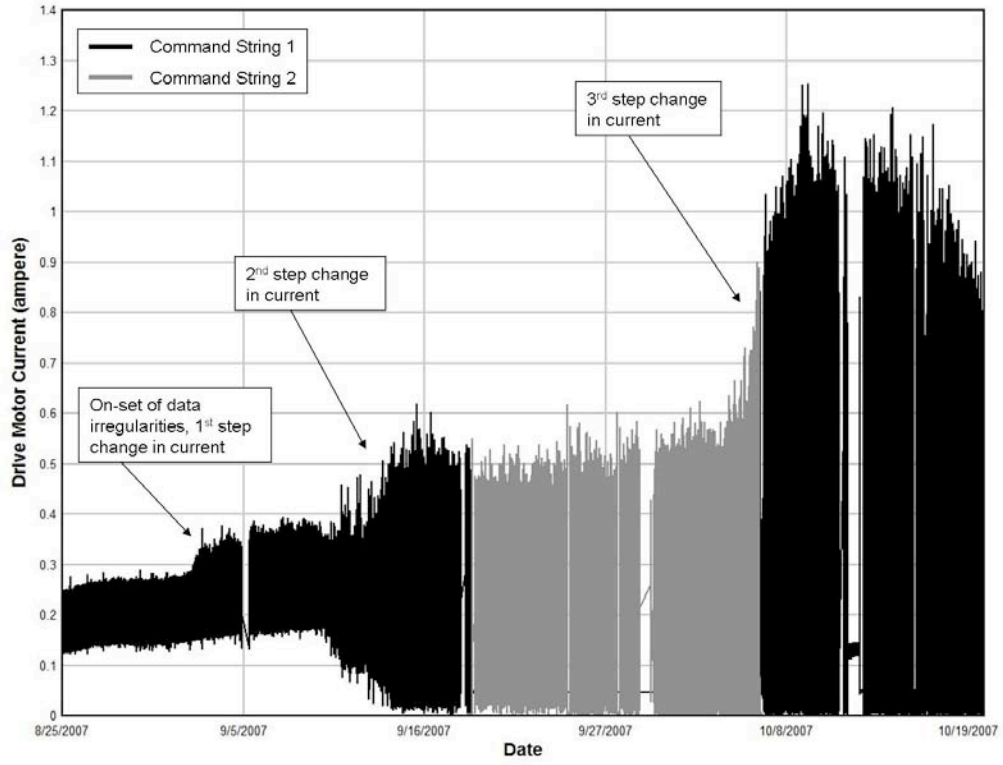

Figure 5. Starboard SARJ Drive Motor Current Changes during the Course of the Anomaly Investigation

In order to fully characterize the joint drag, an on-orbit test was executed. The objectives of the test were to take the controller software out of the loop and directly measure joint drag for all angular positions of the joint. The test objectives were accomplished by operating the mechanism in a mode of operations called “Torque as Stepper” (TAS), which does not utilize the controller loop. In TAS mode, the operator keys in a level of commanded current. The procedure for the test had the operators iteratively step up the amount of current requested until the mechanism began rotating. This was done in 30 degree increments so as to cover all angular positions of the joint. The TAS test confirmed conclusively that the controller was not contributing to the current spikes and that the high drag condition existed across the entire circumference of the joint, although some areas were worse than others. During the test, drag levels ranged between 2380 N·m (1760 ft·lbf) and 2860 N·m (2110 ft·lbf).

The anomaly investigation team was confident that increased joint drag was the source of the data anomalies, however, the source of the drag was unknown. An EVA task was planned on the upcoming Space Shuttle mission to investigate the nature and source of the suspected mechanical drag.

Extra Vehicular Activity and Mechanism Inspection

The goal of the EVA inspection was to look for a “smoking gun” that could have led to the off-nominal data trends. Specifically, the crew was asked to inspect the thermal covers shrouding the joint (Multi Layer Insulation, or MLI, covers) and the bolts that serve as the structural attachment between the MLI covers and the SARJ. This inspection would have revealed any evidence of a micro-meteoroid strike or of some interference between the MLI covers and the rotating half of the SARJ mechanism. Additionally, the crew was asked to inspect the launch restraint fittings to determine if there was any interference with the MLI covers. If time permitted, the crew was also asked to remove a MLI cover to inspect the bearing races and TBAs.

Nothing off nominal was noted during the external survey. The crew had sufficient time to remove a MLI cover for additional inspection. Upon removing the cover the astronaut immediately noticed that there were fine metal shavings across the outboard bearing race surface. Additionally the astronaut noted that the TBA roller housing was acting as a magnet and collecting metal shavings. Samples of the debris collecting around the TBA housing were gathered and returned to ground for analysis (results discussed below). A characteristic picture of the condition of the mechanism can be seen in Figure 6. The outboard race ring, and specifically the outer canted surface, appeared discolored and mottled and there was debris on much of the surrounding hardware.

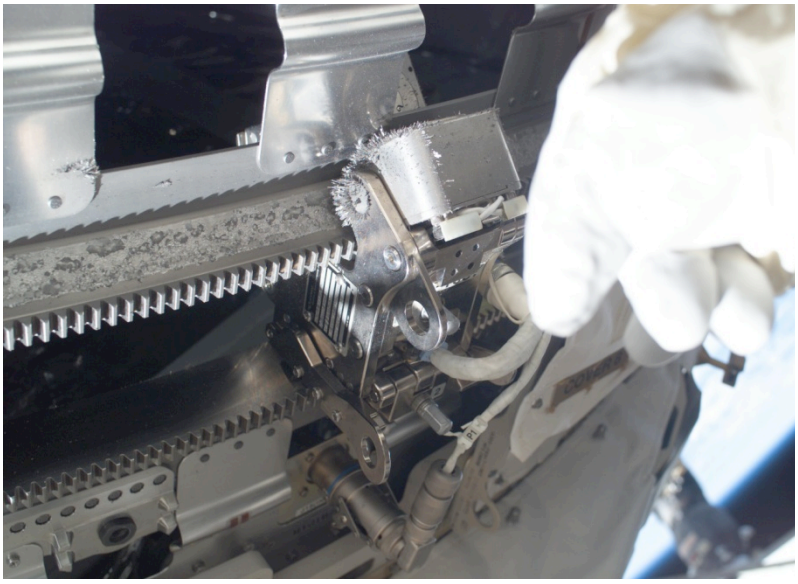

Figure 6. Astronaut Inspecting the Starboard SARJ During an Extra Vehicular Activity

The root cause of the damaged bearing race was not immediately known. It was clear, however, that the mechanism was mechanically damaged and operating in a significantly degraded condition. There was concern that continued operation could exacerbate the problem. Also, the vibrations caused by rotating the joint had become severe enough that accelerated hardware fatigue was a concern. The anomaly investigation team recommended that operation of the Starboard SARJ be halted immediately until the root cause of the anomaly was known.

After seeing the damage on the Starboard SARJ, engineers requested an inspection of the Port SARJ. It appeared to be operating as expected based on telemetry review. The inspection would provide a point of comparison to the Starboard SARJ as well as a baseline image of the mechanism. The Port SARJ

inspection was executed on the following EVA. The astronaut determined that the Port SARJ race rings looked pristine. The inspection confirmed that the damage was confined to the Starboard SARJ. Figure 7 shows a picture of the mechanism taken during the inspection. There is no apparent damage or debris accumulating around the bearing race surfaces or the TBA.

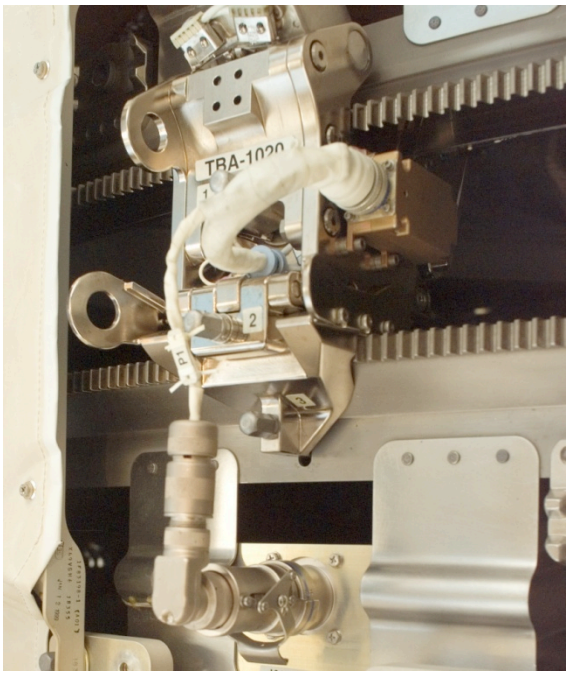

Figure 7. Astronaut Inspection of the Port SARJ During an Extra Vehicular Activity

Lessons Learned

The source of the anomalous data signature was determined less than eight weeks after its genesis. During this period of time the mechanism continued to operate and damage to the bearing race propagated around the entire circumference of the ring. It is possible that if the source of the anomaly had not been discovered, the damage would have progressed further (affecting one of the undamaged bearing surfaces). In hindsight, the anomaly investigation deserves further scrutiny to assess which diagnostic approaches were most effective, and whether any improvements could have been be made to the anomaly investigation process or the health monitoring system.

The best data came from a hands-on visual inspection of the suspect mechanism. For many spaceflight mechanisms, this is not feasible, or comes at an extremely high cost. On-orbit testing also provided an effective means of exonerating specific components as well as characterizing the mechanism performance. A systemic review of all possible contributing factors and appropriate test strategies should be developed immediately after an anomaly is identified.

Additional instrumentation on the mechanism would have aided in diagnosing the anomaly. Strain gauges and accelerometers mounted directly to the TBAs would have been extremely useful. There are strain gauges on the SARJ system but none that measure local deflections at the bearing housings. The SARJ system is susceptible to high tractive forces (addressed in detail in the proceeding sections) which would have been picked up on locally mounted strain gauges. There are accelerometers on the ISS truss but these are not part of the SARJ monitoring and diagnostic system. Ground development testing indicated that the SARJ system was susceptible to debris generation. Accelerometers would provide an indication that debris in excess of expectations was present. A failure modes analysis should lead to the most effective instrumentation and monitoring criteria for a mechanism. Given the susceptibility to debris generation and sensitivity to tractive forces additional instrumentation would have been appropriate for the SARJ.

More consideration early on should have been given to halting operation of the mechanism until the anomalous data signature was better understood. Cessation of nominal operations was not seriously considered until just prior to the EVA inspection because the changes in operating conditions did not represent an immediate threat to successful operation. The system was still effectively tracking the sun with ample torque margin. Instead of focusing on overall system capabilities, it would have been more useful to focus on relative changes in the operational performance. For example, a change in drive motor current from 0.25 to 0.50 ampere represents a change of only 17% in terms of overall torque margin. However, it also reflects a 100% increase in joint drag. This jump in required current should have caused significant enough concern to stop operating the mechanism. Changes relative to previous operational data, or data from the rest of the hardware fleet, are more indicative of hardware issues than changes relative to overall system capability.

Anomaly Root Cause Investigation

A team was formed immediately after the EVA inspection of the Starboard SARJ revealed significant damage to the bearing surface. The team was made up of individuals from NASA Johnson Space Center (JSC), Kennedy Space Center (KSC), Marshall Space Flight Center (MSFC), Glenn Research Center (GRC), Goddard Space Flight Center (GSFC), NASA Engineering and Safety Center (NESC), The Boeing Company, Lockheed Martin Space Systems Company (LMSSC), ATK, and Purdue University. The teams charge was to determine the root cause of the anomaly, determine a corrective action for the damaged mechanism, and determine appropriate recurrence controls for the undamaged (Port) SARJ.

The debris samples taken during the EVA inspections were analyzed in detail by Boeing Houston and NASA JSC and KSC materials and process teams [2]. The analysis yielded several key findings. First, the debris was primarily composed of the case material. Second, the debris thickness showed that the damage did not extend into the core material. And third, the morphology of the debris indicated that the damage was initiated via subsurface spalling. It was not immediately clear to the anomaly investigation team what conditions would generate sufficient stresses to cause the premature case spalling observed.

The anomaly team created a fault tree to aid in the search for the root cause of the damage and to focus in the areas that were critical for investigation. The focus areas were software, hardware, and operations. The fault tree yielded over 350 events that were studied individually. The fault tree events were closed by providing analysis, testing, simulation, or a combination of these. The closure process for the fault tree required that events be combined in a worst-case fashion. A review of fault tree events led to the identification of a set of critical variables for this anomaly. The critical variables were determined to be roller misalignment, lubrication selection and roller/race ring friction, bearing material properties, and applied loading. The team evaluated the interdependencies between the critical variables to determine the most probable root cause of the anomaly.

TBA Roller Misalignment

The TBA roller design causes a pushing action on the roller as the SARJ rotates. This design does not auto correct for roller misalignments as a castoring, or pulling, design would [3]. Misalignment is inherent to any design and manufacturing process. The trundle bearings used match drilled assembly procedures to minimize tolerance build-up and associated roller misalignment. Actual misalignment was not measured on individual units as part of hardware acceptance. After the anomaly had occurred, roller misalignments were measured at MSFC using a coordinate measuring machine as part of the root cause investigation [4]. The measurements showed that the trundle bearing misalignments were all within tolerances (±1 degree). Nevertheless, coupled with high friction, the misalignments were large enough to generate detrimental thrust loads on the roller bearings.

Lubrication Selection and Roller/Race Ring Friction

Gold lubrication was the design choice to mitigate the frictional loads caused by these misalignments in both the TBA and DLA rollers. Test data obtained as part of the SARJ Anomaly (discussed in further detail below) show that a gold film on the trundle bearing rollers could maintain a coefficient of friction of

approximately 0.2 between the TBA rollers and race ring [5]. Nominally, a coefficient of friction of 0.2 ensures that the SARJ system maintains dynamic stability, which allows the race ring to react loads distributed along the full contact patch of the trundle bearing rollers. However, an instability arises when the ratio of thrust load to normal load rises above a critical value of 0.4. At this level of friction, an overturning moment caused by small misalignments in the roller, and subsequent thrust forces, cause the trundle bearing roller to tilt about its camber axis. The roller tilt causes a decrease in the roller race contact and an associated increase in stress at the contact. Test data determined that friction levels in excess of 0.4 are expected if no lubricant exists in the bearing contact, provided that sufficient roller misalignments are present [5].

Bearing Material Properties and Susceptibility to Spallation

The anomaly team postulated that increased friction between the roller/race interface could cause a stress field with the maximum shear stresses at the nitride case/15-5PH core interface. The team also determined that the solid film gold lubricant was not properly adhered to the rollers [6]. Without the gold lubricant in place, the system becomes susceptible to increased shear and normal stresses. The high shear stresses at the case/core interface could lead to subsurface initiated spalling of the case material. Multiple tests were performed over several months in an attempt to reproduce this failure mechanism. Tests performed at the LMSSC facilities in Sunnyvale on a Trundle Roller Rig were successful in recreating the spalling effect observed on-orbit [7]. The test rig loaded a 440C roller against a nitrided 15-5PH coupon. The roller was then rolled in a reciprocating motion along the coupon's surface. Figure 8 above shows a test coupon from the rig. The inset in the figure shows an example of a "fingernail" type spall. Spalls of this type were also noted in on-orbit inspection photos.

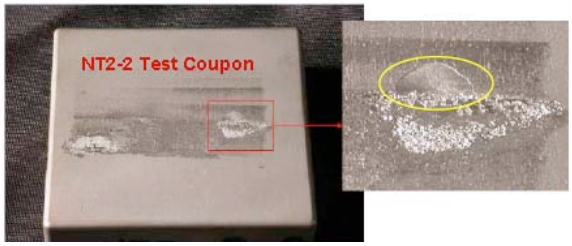

Figure 8. Trundle Test Rig Coupon Showing Fingernail Type Spalling [7]

Applied Loading

The Trundle Test Rig confirmed that subsurface spalling could be induced in the SARJ bearing materials given sufficiently high stress conditions. Additional work was required to validate that the TBA roller kinematics were capable of generating the high stresses required given the expected loading conditions.

A dynamic simulation was developed to perform analysis of the SARJ trundle bearings. The purpose of this simulation was to quantify the loads between each of the trundle bearing rollers and the race ring. The simulation included the race ring deformation caused by the thermal environment, the stiffness of the trundle bearing itself, and the stiffness of the inboard and outboard trusses of the ISS. It also included the structural flexibility of the ISS trusses. The simulations were used to perform parametric studies in support of the closure of the SARJ Fault Tree events. The simulation used traction data obtained from NASA GRC testing for the contact between the race ring and the TBA rollers both with and without gold coating. The simulation was used to estimate the loads at the roller to race ring interface and to illustrate the kinematic behavior of the TBA rollers. The development and results of this simulation are discussed below

Analysis of Roller Edge Loading

The effect of small angular misalignments on rolling traction forces has been studied by a number of investigators, as summarized by K.L. Johnson in [8]. Solutions to the governing equations of rolling have been developed in closed form for a few geometries, and powerful numerical methods have been developed to address the problem for more general application. These methods are important for the present investigation because the angular misalignment of the trundle bearing rollers can lead to dramatic changes in the loads and stresses on the race ring surfaces.

The mistrack or “toe” angle of a TBA roller is the misalignment of the roller due to rotation about an axis normal to the race ring surface. The existence of some small mistracking angle is inherent in the hardware build process. The metrology laboratory at MSFC performed detailed measurements of the mistrack angle of the Starboard SARJ TBA rollers after they had been returned from orbit. Mistracking between the roller and race creates a friction force on the roller in the thrust direction, denoted Q in Figure 9. This yields a moment about the camber axis, which is reacted by the normal load between the roller and race. As the magnitude of the thrust friction increases, the load distribution on the roller becomes unevenly distributed to react the induced moment. The distance *d* in Figure 9 denotes the lateral distance from the camber axis to the center of normal pressure of the contact. In stable tilting, the distance *d* increases with increasing camber tilt, offsetting the camber moment generated by an increasing thrust friction *Q*. However, after a certain camber angle threshold is reached, *d* begins to decrease with increasing camber angle, causing the roller to enter into unstable tilting. The analysis and inspection of the Starboard SARJ TBAs shows that the outer canted rollers remained in the regime of stable tilting during the time when the race ring was being damaged.

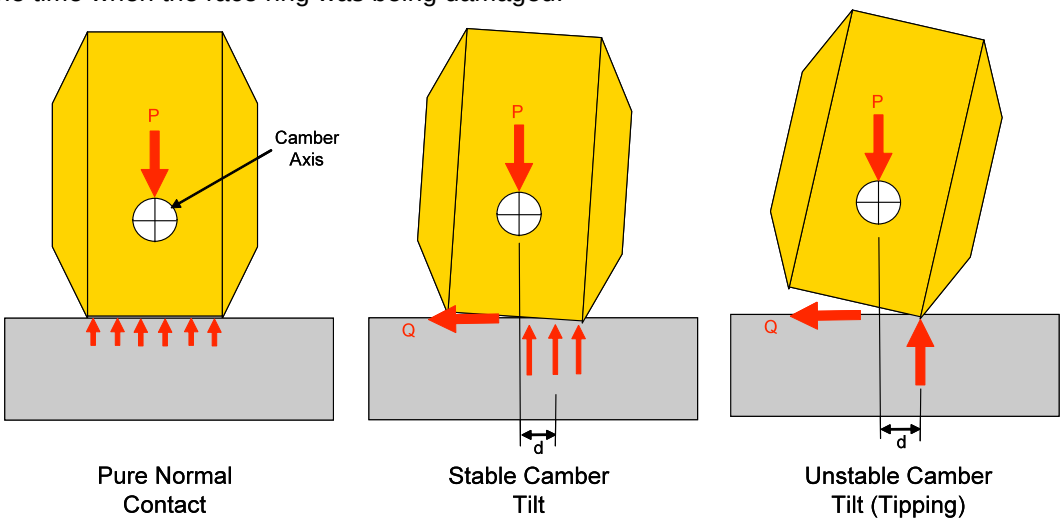

Figure 9. Trundle Bearing Roller Stability

In order to investigate the effect of roller mistracking on the contact forces, a numerical boundary element analysis tool was developed by researchers at Purdue University and Boeing. This tool was rigorously validated against closed form solutions and also shows excellent agreement with the traction results obtained through testing at Glenn Research Center (GRC) [5]. GRC was able to quantify the friction-mistracking relationship in a Vacuum Roller Rig (VRR). The VRR replicates the flight-like rolling interface and materials in a vacuum environment. A comparison between traction curves developed by test at GRC and via analysis is shown in Figure 10. One will note that the analytical results closely match the test data. It is also worth nothing that the VRR rollers do not have identical degrees of freedom to the TBA rollers and therefore the TBA rollers must be addressed by a modified thrust curve (discussed below, see Figure 13).

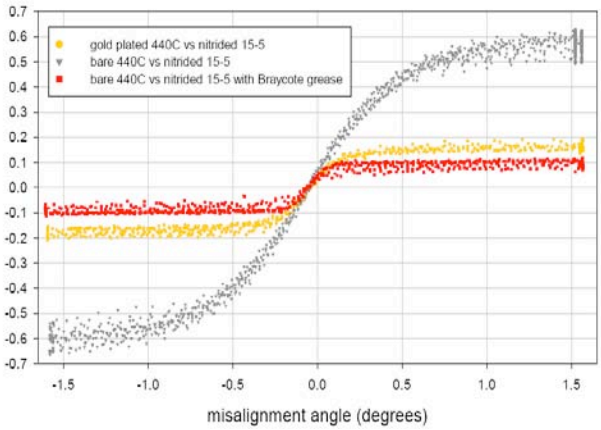

Figure 10. Comparison of Thrust Curves from Analytical Results and VRR Test Data [5]

Figure 11 shows the transverse shear traction distribution on the GRC test rollers for a representative misalignment case. The plot on the left shows that the contact area is divided into regions of stick and slip. The stick region, shown in green, is located at the leading edge of the contact. As the unstressed material of the test rollers enters into the contact patch, the shear deflections and tractions between the two rollers build until the shear tractions reach the limiting value of friction defined by the coefficient of sliding friction, μ, times the normal pressure. As material moves through the trailing end of the contact, slipping occurs between contacting points on the rollers, and the shear tractions remain at the limiting value of friction.

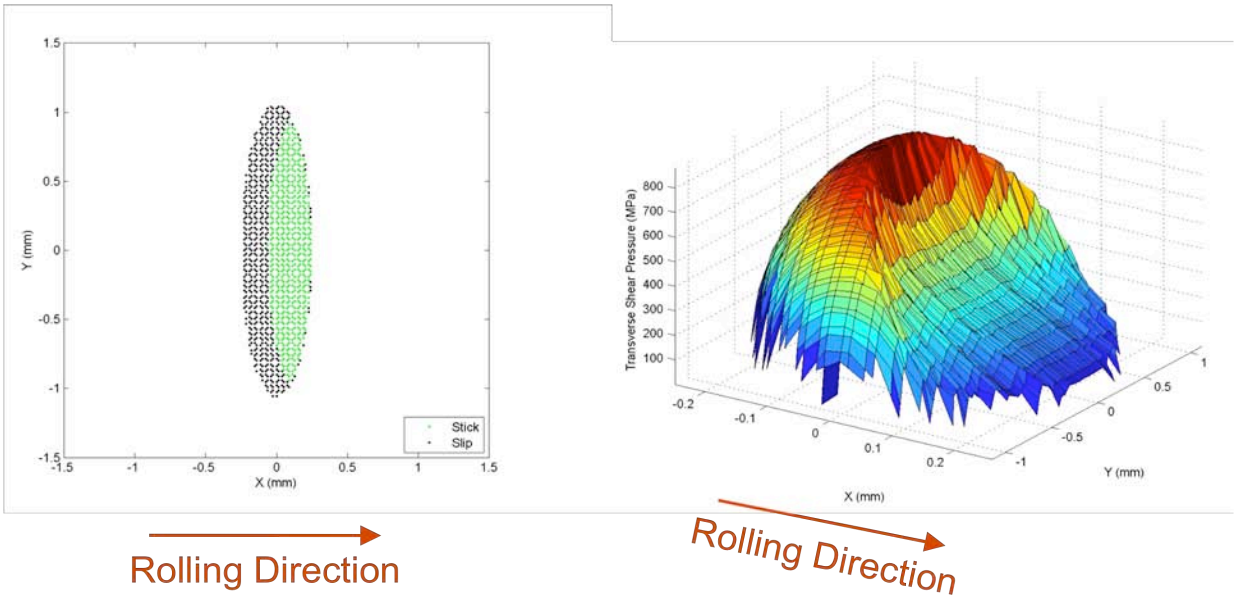

Figure 11. Shear Traction Distribution for GRC Test Rollers, *Q/P* = 0.4

For increasing mistrack angles, the stick region gradually decreases in size until the total thrust load equals μ times the normal load, at which point the entire contact region is in slip. For small mistrack angles such as those observed on the Starboard SARJ TBAs, the rollers remain in partial sliding, and the total frictional force is less than the limiting value of sliding friction.

The tractive phenomena in the flight TBA rollers are analogous to those in the GRC test rollers, with the exception that the TBA rollers have an additional camber degree of freedom. The flight TBA rollers also have a flat profile that transitions to a 1.5-mm (0.060-in) blend radius at the edges of the contact. As a

result, the size and shape of the contact patch for a TBA roller vary dramatically depending on the thrust loading and camber angle of the roller. The contact patch dimensions are plotted in the left portion of Figure 12 for increasing values of thrust load. This plot shows that as the TBA roller tilts on edge due to the thrust loads, the area in contact with the race ring is reduced. The right portion of Figure 12 shows that the average normal contact pressure increases dramatically as a result of the reduced contact area.

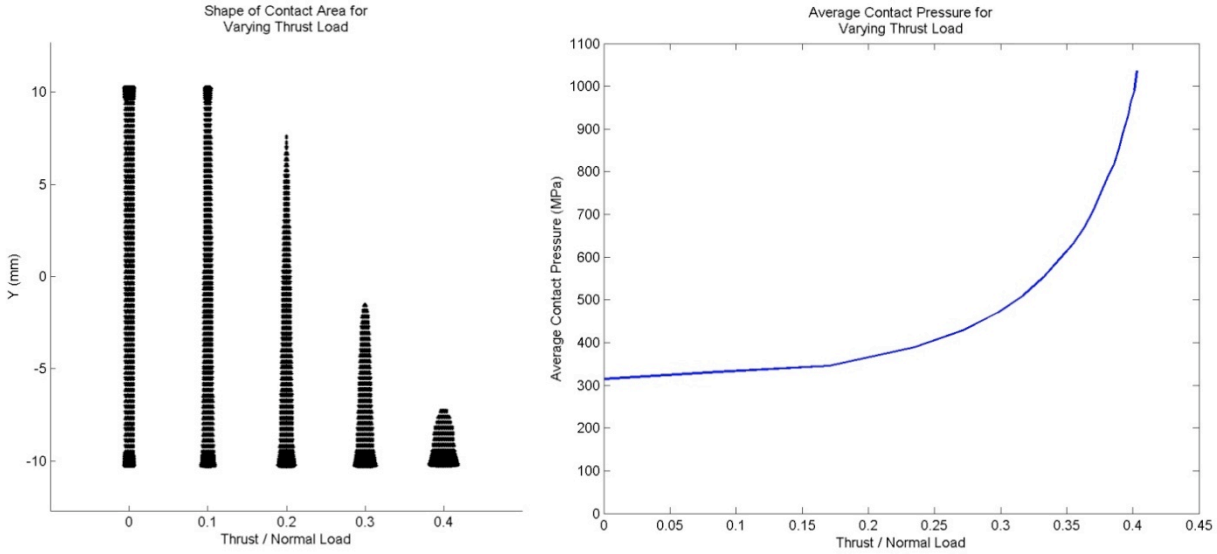

Figure 12. Contact Patch Dimensions and Average Contact Pressure for TBA Roller

In the study of rolling contact mechanics, the relationship between the transverse rolling creep (related to the mistrack angle) and the traction ratio *Q/P* is known as the traction curve. The analysis of the SARJ TBA rollers found that the shape of the contact patch caused by cambering has an influence on the traction curve for the roller. This effect is such that as a TBA roller begins to tip about its camber axis, the frictional loads are less severe than they would otherwise be, thereby mitigating the tipping phenomenon. The blue dotted line in Figure 13 shows the traction curve for the flight TBA roller if the camber axis were fixed at 0°. The red dotted line shows the traction curve if the camber axis were fixed at 2°. In the actual TBA, where the camber axis is free to rotate, the traction curve follows the 0° fixed camber curve for small mistrack angles. However, for larger mistrack angles the changing geometry of the contact patch causes the thrust friction loads to be less severe than in the fixed camber case, as shown by the solid black line in the figure. Despite this phenomenon, thrust loads as high as 0.4 times the normal load can be generated with mistrack angles less than 0.5°.

Detailed measurements and tolerance analysis of the Starboard SARJ TBAs identified an approximate worst case mistrack angle of 0.36°. The normal and shear pressure distributions at the contact are shown in Figure 14 for that mistrack case. As a result of camber tilting, only about one quarter of the width of the roller is in contact with the race ring surface. The resulting stresses at the interface between the race ring case material and the parent material were found to exceed the yield strength of the parent material.

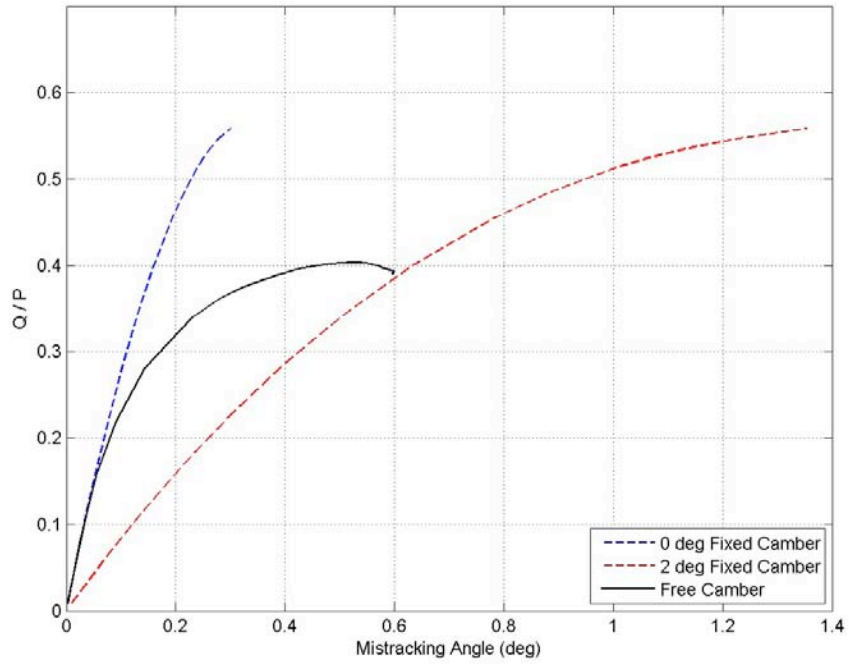

Figure 13. Traction Curves for Outer Canted TBA Roller

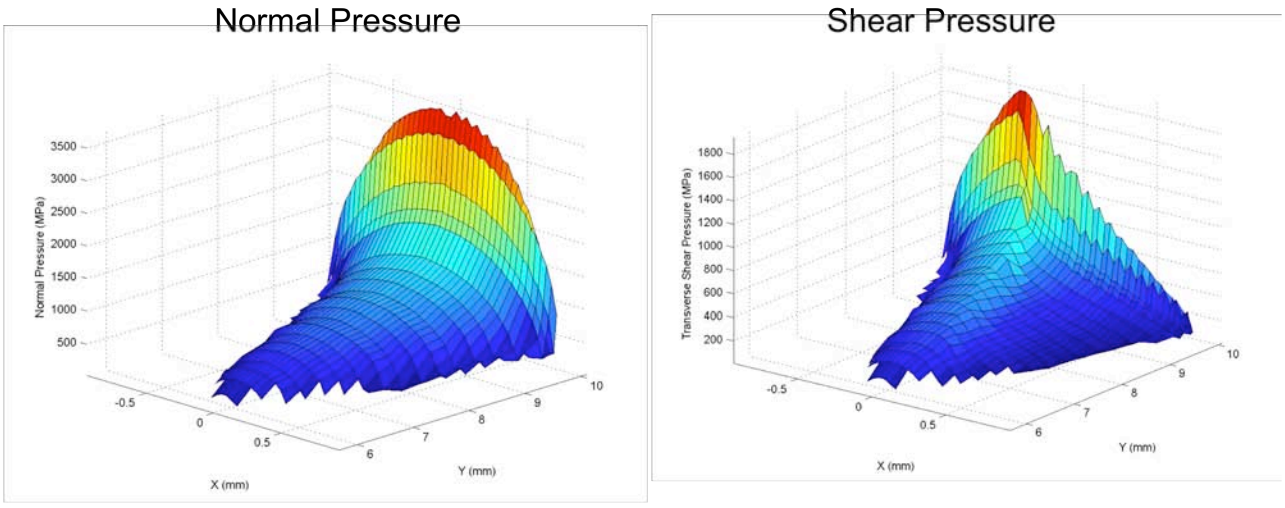

Max Normal Pressure: 3.67 GPa
Total Normal Load: 3.66 kN

Max Shear Pressure: 2.83 GPa
Total Shear Load: 1.41 kN

Figure 14. Distribution of Normal and Shear Pressure for 0.36° Mistracking, TBA Outer Canted Roller

In addition to concentrating the contact pressures at the roller edges, frictional thrust loads due to mistracking also have the effect of increasing or decreasing the normal loads on adjacent rollers. Depending on the specific combination of roller mistrack angles and the direction of SARJ rotation, it is possible for the race ring's triangular cross-section to be wedged in between two of the TBA rollers. This wedging action is analogous to a positive feedback loop. Frictional loads on the Datum A and outer canted rollers lead to increased normal loads on those rollers, which in turn allow the contacts to generate

higher frictional loads. Photographs of the damaged race ring surface taken by the on-orbit crew support the hypothesis that the initiation of damage occurred under these wedging conditions.

Contact Stress for Flat and Crowned TBA Rollers

The root cause team further found that the bearing edge stresses were exacerbated by the flat, un-crowned profile of the TBA rollers. The roller geometry made the system sensitive to non-Hertzian effects, which gave rise to high pressure points at the edges of the rollers during the initial run-in period of the mechanism. These high pressure points are visible in the contact stress profile of the TBA rollers shown in the left side of Figure 15. Part of the recurrence control plan for the SARJ is to modify the rollers on any spare TBAs to include logarithmically crowned rollers. The logarithmic roller profile is a shape that has been mathematically optimized to eliminate the high pressure points that ordinarily occur at the edges of cylindrical roller bearings.

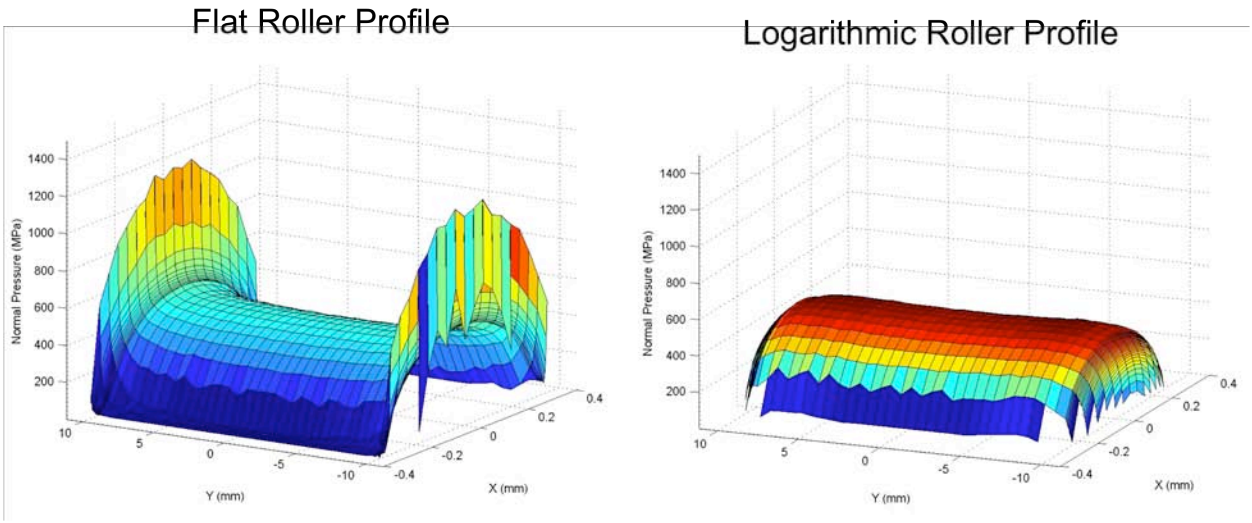

Figure 15. Normal Contact Stress Distribution for TBA Roller, P = 4.36 kN (980 lb)

Root Cause Investigation Conclusions

On-orbit video photographic, visual evidence, and debris samples analyses indicate that the SARJ race ring nitrided layer spalled from the base 15-5 PH steel. The spalling occurred over a period of two and one half months after the Starboard SARJ on-orbit activation. The first signs that the spalling was taking place were manifested through telemetry data that indicated the average operating current of the SARJ was rising from nominal values of 0.15 amp to as high as 0.8 amp.

During this time, the Structural Dynamic Measurement Data System of the ISS was indicating vibrations that were anomalous. These vibrations were later confirmed to be linked to the degrading condition of the SARJ race ring surface. As the race ring surface became progressively rougher over time as a result of the spalling, the vibrations the ISS was sustaining while the Starboard SARJ was rotating were a concern to the structural life of the Space Station. These vibrations were inducing load cycles on ISS hardware that were high enough to be counted in the nominal ISS loads spectrum for structural fatigue.

Testing and analysis indicate that the SARJ race ring surface damage was caused by tractive forces (normal and shear) applied to the race ring surface by the TBA and DLA rollers. Severe loading cases are observed with mistracking angles smaller than the as-measured TBA mistracking angles. Mistracking loads are sensitive to roller edge loading, multiple roller mistracking, direction of mistracking and race ring rotation direction. Analysis indicates that worst loads occur on the gear side of outer canted surface and Datum A surface.

Testing shows that gold, as a solid lubricant, is capable of maintaining a low coefficient of friction (0.2) for mistracking angles higher than the maximum conservatively predicted angle for the TBAs [4,5]. Testing reproduced several visible features of the on-orbit damage [7]. Testing also shows loss of gold adhesion [6]. Using the same roller material as the SARJ TBA, the ion-sputtering process used for the starboard SARJ rollers was re-created and the gold finish was tested. The tests exonerated the gold plating process. However, aging humidity tests indicated that, in time, the gold film would delaminate from the parent material due to corrosive growth on the substrate.

Metallographic analysis was performed to compare the imperfections between the race rings used for the starboard SARJ and the port SARJ. The data indicate that the defect concentrations in the starboard ring nitrided case are approximately six times that of the port nitrided case. The difference in the nitride case defect concentrations makes the starboard SARJ race ring more susceptible to damage initiation and damage propagation caused by high loading. It also may explain the survivability performance of the port SARJ race rings [10].

Anomaly Most Probably Root Cause

The kinematics of the TBA and DLA mechanisms require that the roller thrust loads (related to friction coefficient and mistracking angle) be controlled to ensure stable roller line contact with the race ring surfaces. Inadequate lubrication of the roller/race ring interface combined with roller mistracking angles within specification resulted in thrust loads high enough to cause at least some of the TBA or DLA rollers to edge load as the SARJ rotated. When a roller is edge loaded, the preload on that roller is concentrated on a reduced contact area resulting in high contact stresses and shear stresses in the race ring case and core. These stresses exceed the allowable bearing strength capability of the race ring case and core leading to brittle fracture and spalling of the nitrided layer from the starboard SARJ race ring.

Lessons Learned

As part of the root cause investigation, the build paper was reviewed. Unlike the Port SARJ which was tested in vacuum, the Starboard SARJ was not due to cost considerations. A complex mechanism such as the SARJ cannot be analyzed for break-in performance. Instrumented vacuum testing, particularly for the break-in period, might have yielded indications that the as-built mechanism was not operating nominally. Since the degradation of the Starboard SARJ took place over a short period, during accelerated testing the current increase would have been evident in a very short period of time.

The build-paper investigation also indicates that the testing decisions made for the Starboard SARJ did not accurately account for the friction differences between an ambient and vacuum test environment. The root cause investigation highlighted the sensitivity of the SARJ to small changes in friction. The SARJ Structural Test Article was tested at ambient to verify drive pinion life. The test was not intended to verify system life. However, since the entire system was utilized during the test, successful completion of the test gave a false sense of security regarding system-level life. Recent testing indicates that the vacuum coefficient of friction between 15-5 PH nitrided steel and 440C steel roller is approximately 0.6 [5]. It is now understood that operating the SARJ with coefficients of friction greater than 0.3 increases the risk of roller tilting and resulting damage to the race ring surface.

The root cause investigation also highlighted the importance of correlating testing with analysis and dynamic simulations. Cost-effective and cost-saving simulations can aid the mechanism designer in the understanding of the mechanism performance prior to its fielding. Moreover, mechanism testing should have as a stated objective the correlation of the critical variables of the mechanisms performance. This process can increase the chances of finding phenomena that may be time consuming to test without prior knowledge. The lesson learned here is two-fold and inextricable. A complex mechanism should not be flown into space without testing, nor should it be flown only having been tested. Analysis must be integral to the testing but should not be used in lieu of testing. There are many conditions for mechanism failure that could be understood in a reasonable and cost-effective basis only by analysis.

The damage sustained by the starboard SARJ highlights the importance of sound design and verification practices in the development of complex rotating space machinery. The non-Hertzian contact mechanics of the roller bearing to race ring interface proved to be a crucial detail of the system. Special attention should be given to such effects in the design of bearing systems. The SARJ exhibited high vulnerability to damage during the initial run-in phase of the mechanism's life. The risks incurred during this period can be mitigated through the use of adequate lubrication, crowned rollers, detailed screening of the nitriding process, the implementation of a pre-flight run-in period, and a through understanding of the differences between ambient and vacuum performance. The addition of these elements to the design, verification and operational plans for the SARJ forms the basis for the continued successful use of the mechanism in flight.

On-Orbit Implementation of a Corrective Action

Operations of the Starboard SARJ were severely restricted as soon as the damage was observed. The reduction in operation protected the ISS structure against the vibrations caused by SARJ rotations and against a stall of the mechanism. If the SARJ were to experience an unrecoverable stall, the operational impacts to the ISS would be significant enough to affect future missions and utilization of the station. These potential operational impacts to the ISS warranted corrective action.

The SARJ recovery team concluded that it was a reasonable action to remove debris, to the extent possible, from the damaged race ring and to add grease lubricant to all three bearing surfaces of the race ring. Debris removal was intended to decrease drive motor currents and improve torque margin. The intent of the lubricant was to improve the lubricity between the roller/race interface in order to maintain a coefficient of friction below the critical roller tipping value; the improved lubricity, in turn, would protect the remaining undamage surface from experiencing degradation. Braycote 602EF© was chosen because the base oil has the lowest vapor pressure of all available space greases. It also has molybdenum disulfide which is an excellent lubricant for sliding and capable of handling high loads.

Procedure Development

A preliminary cleaning and lubrication method was developed with inputs from the EVA tools and crew training teams. This method was successfully executed on a small section of race ring during an on-orbit test on the ISS 1J mission. Armed with the lessons learned from the cleaning trials, the team decided to clean and lubricate the entire damaged race ring during the STS-126/ULF2 mission. The team also decided to remove and replace all of the TBAs during ULF2. A significant amount of debris had accumulated on the TBAs, so their replacement would result in additional removal of debris from the joint. This also allowed for the return the original TBAs for inspection to assist in the root cause investigation.

The cleaning and lubrication trials showed that the best method to clean the SARJ was to wet the surface with an EVA wipe pre-lubricated with Braycote 602EF© and then scrape the surface with a scraper tool. Lubricating the surface prior to scraping proved to be the best method to contain the loose debris particles and prevent them from being liberated and dispersed throughout the rest of the mechanism while scraping. The final application of lubricant to the surfaces after cleaning was done using a grease gun. The inner race ring surface is not visible to the crew so a unique lubrication tool, called the J-Hook nozzle, was developed by the JSC EVA tool team to allow the crew to lubricate that surface. Photos of the tools used are shown in Figure 16.

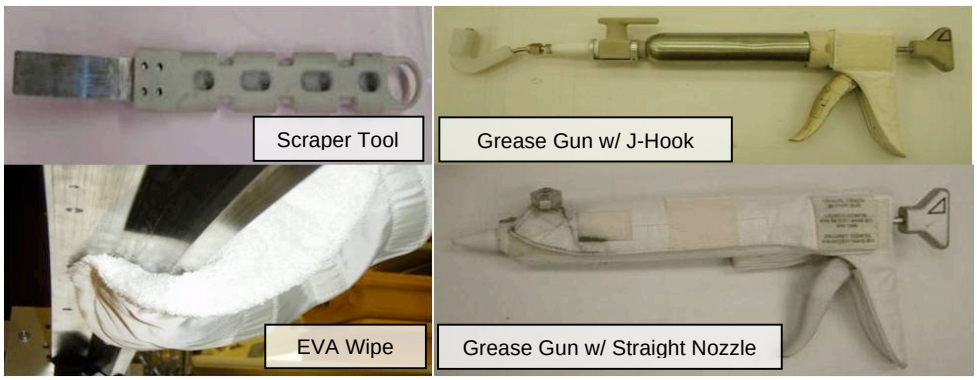

Figure 16. Tools used in SARJ Clean and Lube Operations

While the cleaning methods were developed based upon the on orbit trials, the method to lubricate the cleaned race ring was developed on the ground. A 60-degree section of race ring was used to determine the pattern and quantity of grease to be applied. Based on testing and crew input, it was decided that the best way to apply lubrication to the race ring was to place a single bead of grease down the middle of the roller track. The outer 45 and datum –A- surfaces were lubricated in this manner. The inner 45 race surface was lubricated using the J-Hook nozzle. The J-Hook was designed so the grease would be smeared along the width of the race ring surface and would encompass the roller track of the TBA and DLA rollers. The final grease configuration required residual grease dams on either side of the roller track after the TBA roller had passed over and spread the grease. These repositories of grease on the sides of the track serve as a source of oil that will constantly re-wet the roller track and provide lubrication during subsequent SARJ operations.

Lab tests were also run where grease was added to a race ring surface contaminated with metallic particles similar to the debris retrieved from the SARJ on orbit. These tests showed that the hydrodynamic force generated by the roller passing over the grease was enough to push a majority of the debris out of the roller track. As a result, the addition of lubricant to the damaged race ring serves a dual purpose as a cleaning fluid for any debris left on the SARJ after the cleaning operation. The clean and lubrication operations were successfully completed during ULF2. Figure 17 shows the final application method and grease configuration.

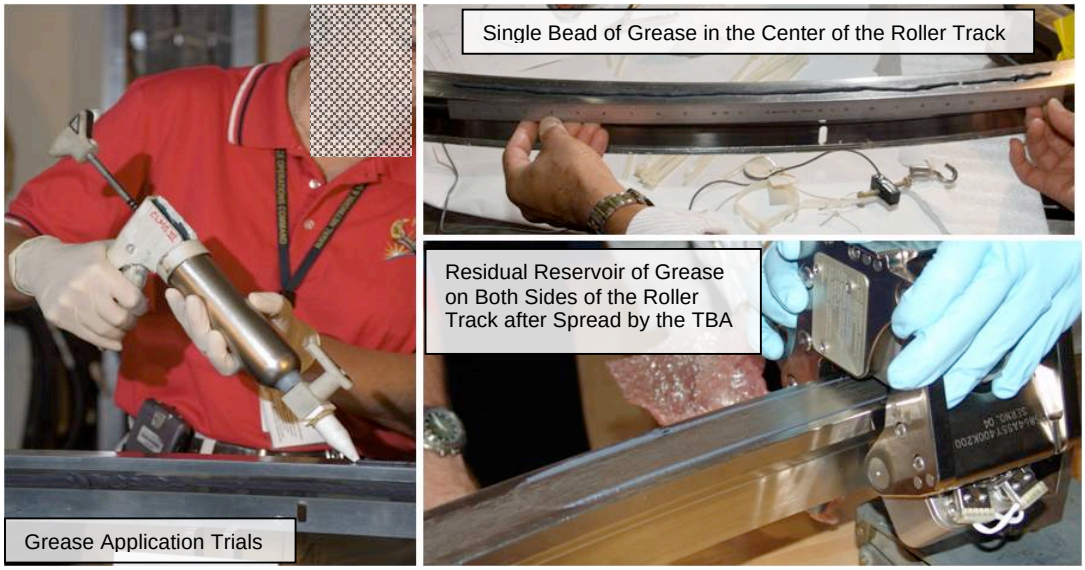

Figure 17. Final Grease Application Methods

Results of Corrective Action

Following the successful cleaning and lubrication of the starboard SARJ, the joint was rotated and the motor drive current was monitored. The motor current decreased immediately from a pre-cleaning and lubrication average of 0.242 ampere to 0.174 ampere. The more critical benefit was the significant reduction in the maximum current levels. The large swing in motor drive current observed prior to the clean and lube operations was mitigated significantly, resulting in a reduction in the maximum current from 0.870 ampere to 0.384 ampere. These results demonstrate that the clean and lube operations were successful in increasing the stall margin in the SARJ which, in turn, maintains operational flexibility of the ISS. These post lube data also compare well with the performance of the starboard SARJ telemetry prior to the anomaly when the SARJ had an average motor current of 0.153 ampere and a maximum of 0.221 ampere. Data plots showing the motor current prior to the clean and lube operations (data taken during the 10A mission), during ULF2 just after the clean and lube operations, and data taken during ULF2 stage operations are shown in Figure 18.

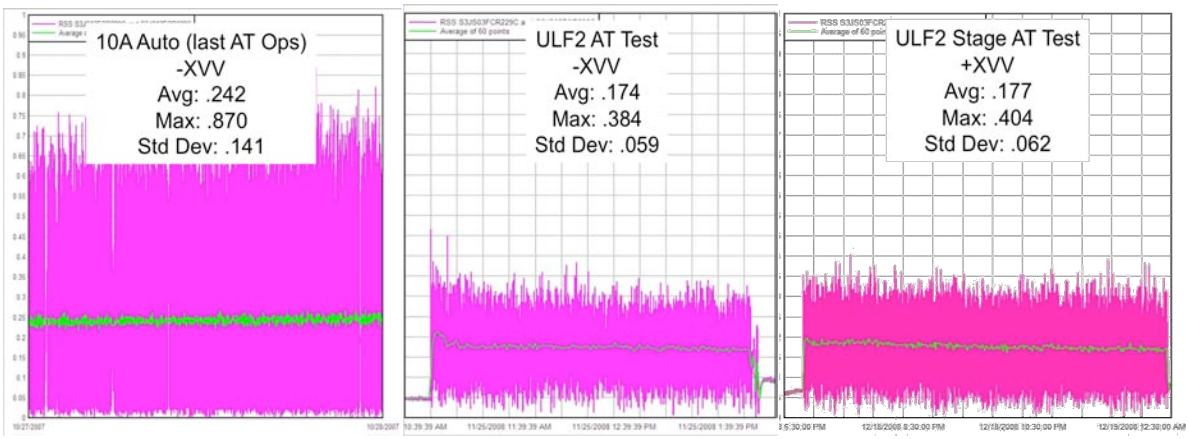

Figure 18. Starboard SARJ Motor Drive Current Comparison Pre and Post Clean & Lubrication

The port SARJ was also lubricated with Braycote 602EF© during Flight ULF2 using the same procedures and tools as were developed for the starboard SARJ. The lubricant was intended to protect the mechanism against damage by the same mechanism as was experienced by the starboard SARJ. Pre and post lubrication data for the port SARJ shows a 20% decrease in average drive motor current, shown in Figure 19. This drop is significant as it indicates that the mechanism pre lubrication was operating in a regime of higher roller/race friction than post lubrication and was therefore more susceptible to damage initiation prior to the application of the grease lubricant.

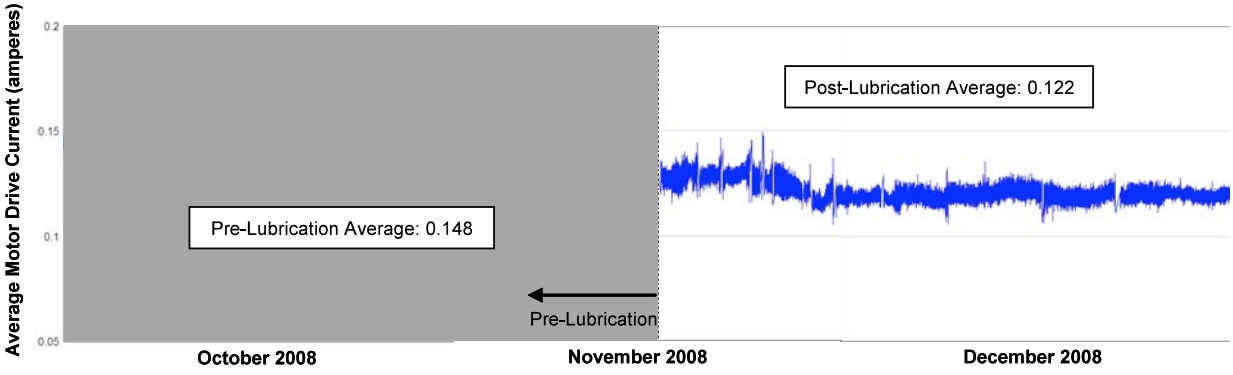

Figure 19. Port SARJ Average Motor Drive Current Comparison Pre and Post Clean & Lubrication

As noted earlier, anomalous structural vibrations were one of the first hints of a problem with the SARJ. The surface of the race ring had degraded significantly and it was not anticipated that the clean and

lubrication tasks would have a significant impact on the vibrations observed on ISS. The accelerometer data after ULF2 showed that the peak accelerations had been reduced significantly. Data plots showing pre and post ULF2 accelerometer data are displayed in Figure 20 and show the dramatic decrease in vibrations to the ISS due to SARJ rotation.

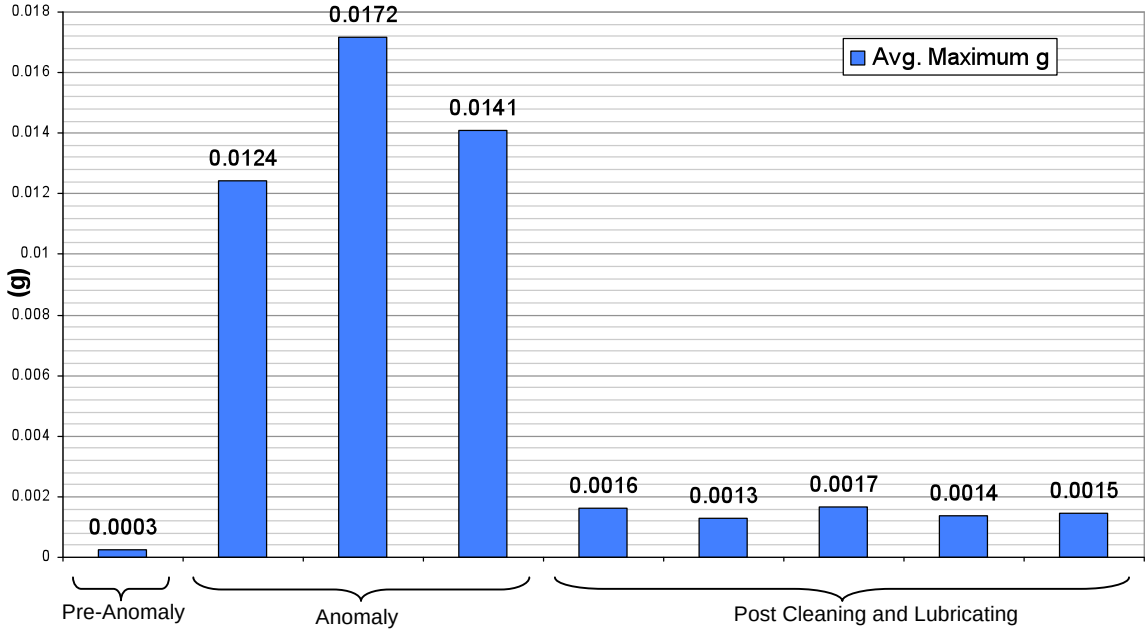

Figure 20. ISS Acceleration Data Pre and Post ULF2 [9]

Lessons Learned

The dramatically improved performance of the SARJ mechanism due to the cleaning and addition of grease to a damaged and contaminated race ring is an important finding for space systems mechanism design. Most directly, these observations can be applied to the design of mechanisms that will, by nature of their intended use, be exposed to high levels of contamination (e.g., mechanisms on lunar or Martian based systems). It is recommended that designers consider adding the capability of re-lubrication and/or cleaning of bearing systems, especially those which be exposed to high debris filled environments.

Conclusions

Anomalous performance of the Starboard SARJ was noted shortly after the mechanism was activated on-orbit. An inspection found that there was debris covering the bearing race of the rotating mechanism. An anomaly team was immediately formed to investigate the issue. Through a series of tests, analysis, and simulations the team determined that the most likely cause of the damage was high friction at the bearing/race ring contact coupled with a susceptibility of the bearing mechanism to an overturning moment on the bearing rollers. Dynamic analysis simulating the contact conditions of the SARJ mechanism, both lubricated and un-lubricated, confirmed that in the un-lubricated condition sufficient stresses occur to damage the race ring. Grease lubricant was applied to the mechanism in order to mitigate the existing damage as well as prevent further damage. Additionally, astronauts removed the debris noted during previous inspections. These actions proved effective as overall joint drag significantly decreased as did structural vibrations caused by operating the mechanism.

The SARJ anomaly investigation and recovery provides several lessons learned both in the arena of diagnosing on-orbit anomalies and in complex aerospace mechanism design and verification. Mechanism design should incorporate proven and verifiable features whenever possible. Features that do not lend

themselves readily to analysis cannot easily undergo the rigorous verification process that aerospace mechanisms demand; for example the TBA roller profile gives rise to non-Hertzian contact effects, which requires advanced analytical methodology in order to recover the stresses. The acceptance program for complex mechanisms should include a run-in period during which the mechanism is operated in the flight environment. This run-in period should be used to correlate analytical models of the mechanism as well as provide a baseline of expected performance for the mechanism while on-orbit. Test correlated and verified models can be used to determine system level sensitivities and potential design problems. Additionally, understanding the sensitivities of the system will allow for the most effective use of instrumentation and monitoring techniques of the mechanism while on orbit. A baseline performance characterization provides ground operators an effective means for gauging the severity of changes in performance after activation. Finally, mechanisms that operate in an environment susceptible to debris contamination should consider inclusion of re-lubrication and cleaning capabilities. These lessons should be utilized by architects of future aerospace mechanisms to yield more robust systems.

References

1. Leger, L. J. & Dufrane, K. (1987). “Space Station Lubrication Considerations.” *21st Aerospace Mechanisms Symposium Proceedings*. NASA-CP-2470.
2. Wright, M. C., Salazar, T., Kim, H., Tucker, B., Lubas, D., Marciniak, P., McDanels, S. (2008, February). “International Space Station (ISS) Starboard Solar Alpha Rotary Joint (SARJ) Expedition 16 EVA 13 and 14 Debris Analysis.” KSC Engineering Directorate, Materials Science Division.
3. Favero, J., Frazier, B., Nielsen, P. (1998, October). “SARJ Dynamic Simulation Analysis and Results.” The Boeing Company. A03-J092-PN-M-9801474.
4. Moore, L.E. “DRAFT SARJ Anomaly Report for Review – STATUS.” Message to Carlos Enriquez. 13 July 2009. E-mail attachment.
5. Krantz, T., DellaCorte, C., Dube, M. (2010). Experimental Investigation of Forces Produced by Misaligned Rollers. *40th Aerospace Mechanisms Symposium Proceedings*. **Manuscript in preparation**.
6. Enriquez, C.F. (2009, September). *International Space Station Solar Alpha Rotary Joint Anomaly Report*. The Boeing Company, International Space Station Program. D684-13412-01.
7. Loewenthal, Stu, Scotty Allen, and John Golden. "Solar Alpha Rotary Joint Anomaly Test Findings: Mechanism Perspective." *Aging Aircraft 2009*. (2009): Print.
8. Johnson, K.L. (2003). *Contact Mechanics*. Cambridge, United Kingdom: Cambridge University Press.
9. Laible, M. (2009). “SSARJ Autotrack Test 5 Results.” The Boeing Company, Houston, Loads and Dynamics.
10. Martinez, J.E. “SARJ DIGS % Area Calculations.” Message to Dr. John Goldon. 01 December 2009. Email attachment.